Article

Dramatic Lockdown Fossil Fuel CO_2 Decrease Detected by Citizen Science-Supported Atmospheric Radiocarbon Observations

Jocelyn C. Turnbull,* Lucas Gatti Domingues, and Nikita Turton

Cite This: *Environ. Sci. Technol.* 2022, 56, 9882−9890

Read Online

ACCESS | Metrics & More | Article Recommendations | Supporting Information

ABSTRACT: COVID-19 lockdowns resulted in dramatic changes to fossil fuel CO_2 emissions around the world, most prominently in the transportation sector. Yet travel restrictions also hampered observational data collection, making it difficult to evaluate emission changes as they occurred. To overcome this, we used a novel citizen science campaign to detect emission changes during lockdown and engage youth in climate science. Citizen scientists collected grass samples from their garden or local park, from which we analyzed the radiocarbon content to infer the recently added atmospheric fossil fuel CO_2 mole fraction at each sampling location. The local fossil fuel CO_2 mole fractions during lockdown were compared with a "normal" nonlockdown period. Our results from 17 sites in five cities around New Zealand demonstrate dramatic reductions in traffic emissions of 75 ± 3% during the most severe lockdown restriction period. This is consistent with sparse local traffic count information and a much larger decrease in traffic emissions than reported in global aggregate estimates of emission changes. Our results demonstrate that despite nationally consistent rules on travel during lockdown, emission changes varied by location, with inner-city sites typically dominated by bus traffic showing smaller decreases in emissions than elsewhere.

KEYWORDS: *fossil fuel CO_2, radiocarbon, lockdown, emissions, citizen science*
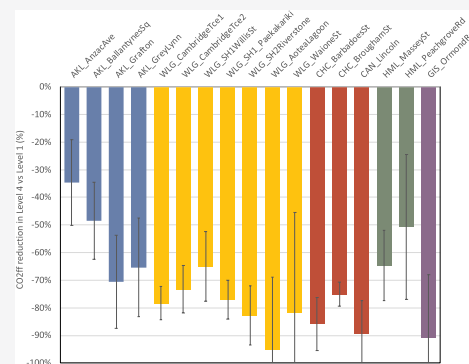
1. INTRODUCTION

The impossibility of accessing sites and collecting samples during COVID-19 lockdown led us to use a novel citizen science campaign to reconstruct fossil fuel CO_2 (CO_{2ff}) emissions from grass samples collected from five cities around New Zealand. While CO_2 emissions have gradually increased over the last decades to about 10 gigatonnes of carbon per year in 2019,[1] the 2020 COVID-19 lockdowns resulted in dramatic, but often short-lived, widespread CO_{2ff} emission decreases.[2,3] Changes in air quality metrics have been evaluated through atmospheric and remote sensing observations at many locations around the world,[4−8] but greenhouse gas changes due to COVID-19 have been challenging to evaluate from atmospheric observations largely because changes in the CO_{2ff} atmospheric enhancement are expected to be modest relative to the large and variable CO_2 background. Thus, the first estimates of CO_{2ff} emission changes were based on the extrapolation of inventories using proxy data.[2,3] Atmospheric observations of CO_{2ff} during COVID-19 lockdowns have not yet been reported, and only a small number of studies have detected changes from atmospheric observations of total CO_2.[9−12]

^{14}C is well recognized as an ideal tracer for CO_{2ff} since fossil fuels have been out of contact with the atmosphere for millions of years, and all ^{14}C initially present has long since decayed radioactively. In contrast, other CO_2 sources contain ^{14}C in roughly the same proportion as the current atmosphere.

Therefore, the ^{14}C content of atmospheric CO_2 can be used to determine the CO_{2ff} content.[13−15]

Plant material provides a natural sampling method to determine the radiocarbon (^{14}C) content of atmospheric CO_2. When plants photosynthesize, they use the carbon from CO_2 to grow, and faithfully record the ^{14}C content of the CO_2 assimilated from the atmosphere. Tree rings, leaves, and other plant material are thus widely used to reconstruct past atmospheric ^{14}C content.[16] Moreover, the first direct evidence that fossil fuel CO_2 emissions were driving changes in atmospheric CO_2 came from ^{14}C measurements in tree rings.[13] While tree rings record the ^{14}C content of the atmosphere for each year of growth,[13] leaves can be used to sample the atmosphere over the shorter period of their growth.[17,18] Grass is particularly useful for short-term sampling because of the rapid growth of the grass blades that can represent just a few days or weeks of growth.[18] Short-lived plant material has thus been widely used to determine atmospheric ^{14}C content

Figure 1. Grass sampling locations around New Zealand (white) and Baring Head clean air site used as background (blue).

and derive local patterns of CO_{2ff} mole fraction in contemporary samples.[17−20]

During New Zealand's most severe lockdown from 26 March to 27 April 2020, termed "Level 4", most people were confined to their family bubble and no travel more than 5 km from home was allowed. Almost all businesses and industries were closed, with only pharmacies, medical services, supermarkets, and petrol stations remaining open. It was not possible to obtain travel exemptions for scientific research. Instead, we initiated a citizen science campaign to allow monitoring of CO_{2ff} emission changes during this unique severely restricted travel period. We recruited citizen scientists from around New Zealand to collect short-lived grass samples from their own lawn, a local park, or a nearby roadside. The weekly samples were collected during lockdown and through until return to near-normal conditions. Each sample was analyzed for ^{14}C content, from which local fossil fuel CO_2 mole fraction was determined, and emission changes inferred.

2. METHODS

2.1. Sample Collection. More than 400 people from around New Zealand signed up to the Great Greenhouse Gas Grass Off initiative, and in many cases, children were the main sample collectors under the guidance of their parents or caregivers. Citizens were asked to choose a local grass patch, ensuring that they did not violate the lockdown travel and social distancing requirements. They were asked to take an initial sample, cutting the grass down to the white roots, and store the dated and labeled sample in a freezer. Each week, they were reminded to collect a new regrowth sample from the same grass, continuing through Level 4 (March 26 to April 27, 2020) to the less restrictive Level 3 (April 28 to May 13, 2020), Level 2 (May

14 to June 8, 2020) and the removal of in-country travel and work restrictions in Level 1 (from June 9, 2020). Participants were encouraged to engage in the science, with regular social media updates explaining the methods and reporting results as samples were measured.

Ultimately, 110 sample sets were submitted to our laboratory, along with many detailed handwritten letters, maps, and photographs. From these, we selected 26 sample sets that contained sufficient samples to track emissions during the full lockdown period and return to normal conditions; were of sufficient quality for ^{14}C analysis; and from locations where substantial local CO_{2ff} emissions might be anticipated.

Seventeen of these sites from five cities around New Zealand (Figure 1) proved to have robust, interpretable CO_{2ff} signals and are presented here. The remaining sampled nine sites are excluded because they either had small to negligible CO_{2ff} signals and therefore emission changes could not be determined with statistical significance or showed large variability in CO_{2ff} during the Level 1 "normal" conditions (Section 2.4). Of the 17 selected sites, four are in New Zealand's largest city (population 1.5 million), seven are in the Wellington region (population 400,000), three in Christchurch (population 400,000), two in Hamilton (population 200,000), and one is in the medium-sized town of Gisborne (population 40,000). All of New Zealand's towns and cities have modest population density, ranging from about 2400 people/km^2 in Auckland to 1000 people/km^2 in Gisborne.

All of these sites are within 20 m of a road; maps of each site are given in Figures S2−S4. The Auckland sites are near urban (AKL_ANZACAve, AKL_BallantynesSq) and suburban roads (AKL_Grafton, AKL_GreyLynn). In Wellington, three sites are

adjacent to motorways or major arterial routes with normally heavy traffic (WLG_SH1Paekakariki, WLG_SH2Riverstone, WLG_AoteaLagoon), and one is at a traffic light intersection at the terminus of a major motorway (WLG_SH1WillisSt). Two Wellington sites are located on the grassed median on an inner-city street, one adjacent to a traffic light intersection (WLG_CambridgeTce1) and the second site about 100 m south (WLG_CambridgeTce2). The seventh Wellington site is on a suburban street (WLG_WaioneSt). Two Christchurch sites are on urban streets (CHC_BarbadoesSt, CHC_BroughamSt), and the third (CAN_Lincoln) is a major arterial route through farmland just outside the city proper. The Hamilton and Gisborne sites are all suburban streets (HML_MasseySt, HML_PeachgroveRd, GIS_OrmondRd).

Citizen scientists were asked to collect samples by harvesting the green grass leaves down to the white roots. The following sample then represents growth during the period since the last sample was collected, typically one week. The growth period of the first sample of each series is not well known but estimated to be the two weeks preceding the sample collection. Harvested grass length varied between 1 and 5 cm. Samples from an individual site were always the same species (having been harvested from regrowth of the same plant), but grass type may differ across different sites. Grass assimilates carbon only during daylight hours when sunlight enables photosynthesis, so each grass sample represents daylight hours for the days since the last sample was harvested. Since we measure the ^{14}C content of assimilated CO_2, varying growth rates at different sites and times do not impact the ^{14}C content and derived CO_{2ff} mole fractions.

The growth period must always be an approximation, as plant growth and CO_2 assimilation vary depending on daylight hours, irradiance, meteorology, and plant growth cycles.[21] For our sampling period, daylight hours gradually decreased each week so that samples collected during Level 1 are biased to a shorter part of the day than those during Level 4. The samples are also biased toward sunny periods. Although we asked citizen scientists to collect the full regrowth each week, it is possible, or even likely, that some samples might include growth from the previous week(s). It is also possible that some fraction of the new growth is derived from carbon assimilated over previous weeks and remobilized into the newly grown grass leaves.[21] Nonetheless, each sample approximates the ^{14}C content of atmospheric CO_2 at that location during daylight hours over the period of sample growth.[17,19,20]

2.2. Radiocarbon Analysis. For each sample, the full length of a grass blade (or blades) was selected. Length varied by sampling site and date, ranging from 1 cm to 5 cm in length. If insufficient weight was obtained from a single blade of grass, multiple blades were combined. Since grass blades grow from the base, by selecting the full length of a blade, each blade should represent the full time period since the last sample was collected, noting the sampling biases due to when carbon is assimilated as discussed in Section 2.1.

Selected samples were prepared and measured by standard ^{14}C techniques,[18] which included an acid wash to remove surface material, combustion to CO_2 gas by elemental analyzer, and reduction to graphite over iron catalyst. ^{14}C measurement was by accelerator mass spectrometry. Reported uncertainties were assessed by the variability of replicate samples prepared from separate grass blades collected at the same site and date. We found an overall repeatability of 2.1‰ from six replicate samples encompassing both clean air and polluted sites (Figure S1). This is somewhat higher than the assessed ^{14}C measurement

uncertainty of 1.7‰ and indicates that there is a modest amount of additional uncertainty introduced by CO_2 assimilation or grass collection. We increased the assigned uncertainties by 1.2‰ (added in quadrature) to include this additional source of variability, resulting in final ^{14}C uncertainties of 2.0−2.2‰ (Supporting Dataset).

2.3. Determination of CO_{2ff}. CO_{2ff} was determined from measured $\Delta^{14}C$[14,17,22] such that

$$CO_{2ff} = \frac{CO_{2bg}(\Delta_{obs} - \Delta_{bg})}{\Delta_{ff} - \Delta_{bg}} - \beta \tag{1}$$

where CO_{2bg} is the background CO_2 mole fraction, in this case determined from the mean CO_2 value at Baring Head, near Wellington (Figure 1) over the full sampling period. Δ_{obs} is the observed $\Delta^{14}C$ in the grass sample. Δ_{ff} is the $\Delta^{14}C$ of fossil fuel CO_2, −1000‰ by definition for ^{14}C-free material. Δ_{bg} is the $\Delta^{14}C$ of background air for the same time period, for which we also used the mean measured $\Delta^{14}C$ of 7.1 ± 0.5‰ at Baring Head for March−July 2020 (extended dataset available at https://gaw.kishou.go.jp/).[23] There is a slight, but not significant, downward trend in the Baring Head $\Delta^{14}C$ values (Figure 2). We tested the impact of varying the background to account for this trend, but this did not significantly alter the calculated CO_{2ff} values.
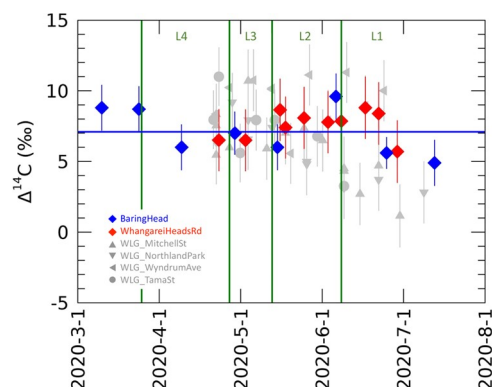
Figure 2. $\Delta^{14}C$ measured at five sites with little local fossil fuel CO_2 influence. Green lines indicate lockdown levels Changes in lockdown level from highest (L4) to lowest (L1) are indicated by the green vertical lines. The blue line indicates the assigned background $\Delta^{14}C$ value derived from Baring Head $\Delta^{14}C$ during measurements. Error bars are the assigned one-sigma uncertainty as described in the text.

β is a correction for the slightly elevated $\Delta^{14}C$ in heterotrophic respiration, and we use a value of −0.5 ± 0.25 ppm in CO_{2ff}.[22] To test this correction, we used grass samples collected for this study from a rural site near Whangarei (Figure 2) and Level 4 and Level 3 at four windy suburban sites in Wellington (WLG_WyndrumAve, WLG_TamaSt, WLG_MitchellSt and WLG_NorthlandPark, Figure 2) which together had mean $\Delta^{14}C$ of 8.0 ± 0.3‰. Assuming no CO_{2ff} influence in these samples, the slight elevation in $\Delta^{14}C$ with respect to Baring Head was used to diagnose the heterotrophic respiration bias term as −0.4 ± 0.2 ppm, comparable to the canonical value of −0.5 ± 0.25 ppm. We note that WLG_MitchellSt and WLG_NorthlandPark do appear to have a modest CO_{2ff} signal during Level 2 and Level 1, and these data are not used in the background analysis.

2.4. Estimation of CO_{2ff} Emission Rate Changes from CO_{2ff} Mole Fraction Observation. Ultimately, we are

Figure 3. continued

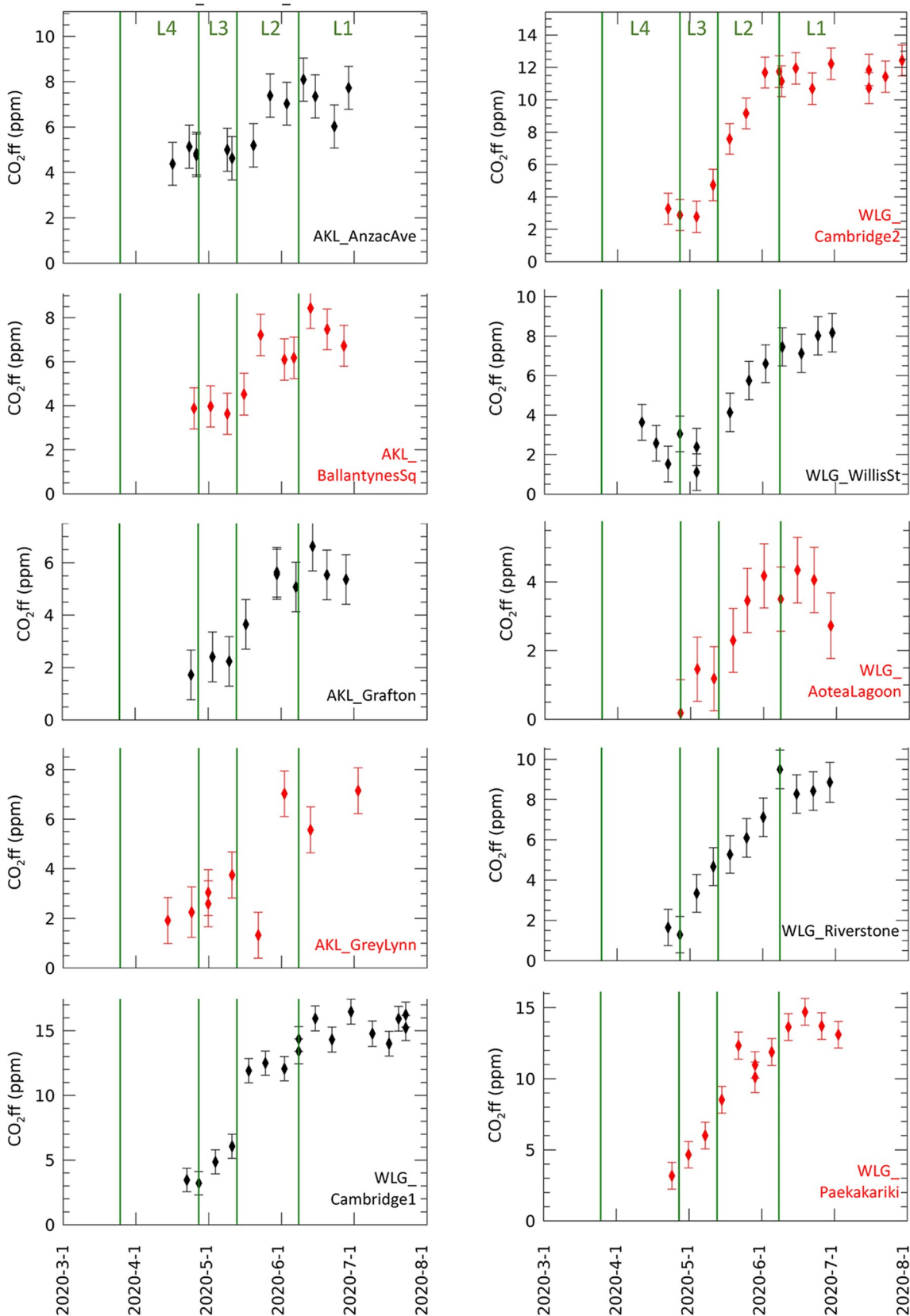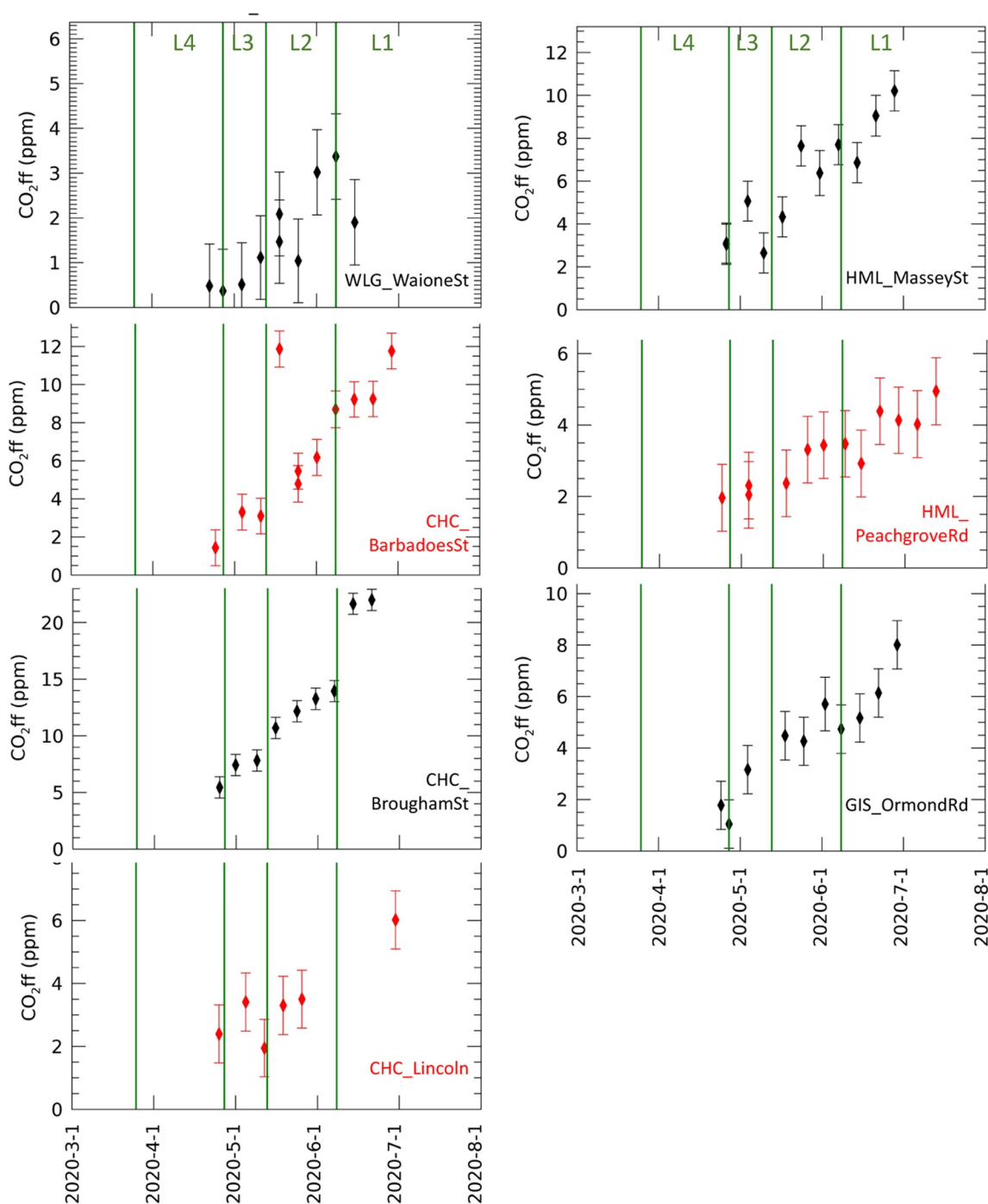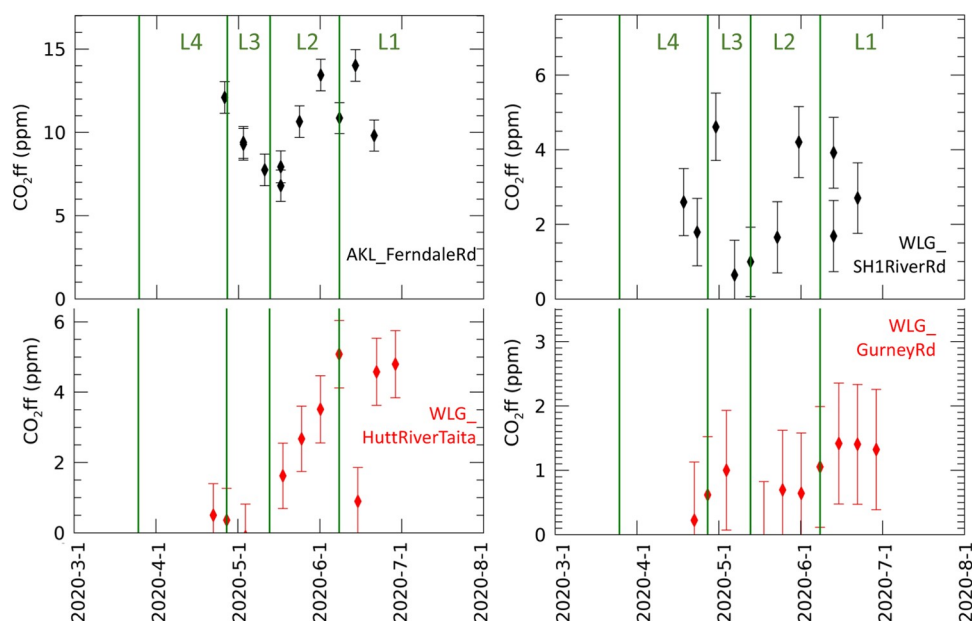**Figure 3.** Observed CO_{2ff} mole fractions determined from ^{14}C measurements in grass for 17 sites in five cities around New Zealand: Auckland (AKL), Wellington (WLG), Christchurch (CHC/CAN), Hamilton (HML), and Gisborne (GIS). Changes in lockdown level from highest (L4) to lowest (L1) are indicated by the green vertical lines. Error bars are the assigned one-sigma uncertainty as described in the text.

interested in the CO_{2ff} emission rate, whereas our observed CO_{2ff} from the grass samples is a function of both the local CO_{2ff} emission rate and the meteorological conditions transporting emitted CO_{2ff} to the grass location.

First, we estimate the area of influence for each grass sample. Grass necessarily grows within a few centimeters of the Earth's surface. The atmospheric flow this close to the ground, particularly among rapidly growing grass, is difficult to assess and made even more complex at urban sites with nearby buildings, trees, and other topographic features.

Still, we used the WindTRAX Lagrangian stochastic model[24] to estimate the relative influence of nearby sources. Local wind data was available at only one of our sites, which was directly adjacent (within 5 m) to an air quality monitoring station (WLG_SH1WillisSt). We choose three representative weeks of wind data and ran the WindTRAX model for a receptor 50 cm above the surface. The model estimates that emissions within 20 m of the grass will have a 10-fold larger influence than those 50 m away, indicating that the closest sources will strongly dominate the observed CO_{2ff} mole fraction. All 17 selected sites were

Figure 4. Observed CO_{2ff} mole fractions for four sites that were rejected from analysis due to either: variable CO_{2ff} during Level 1, or signals that are too small to interpret.
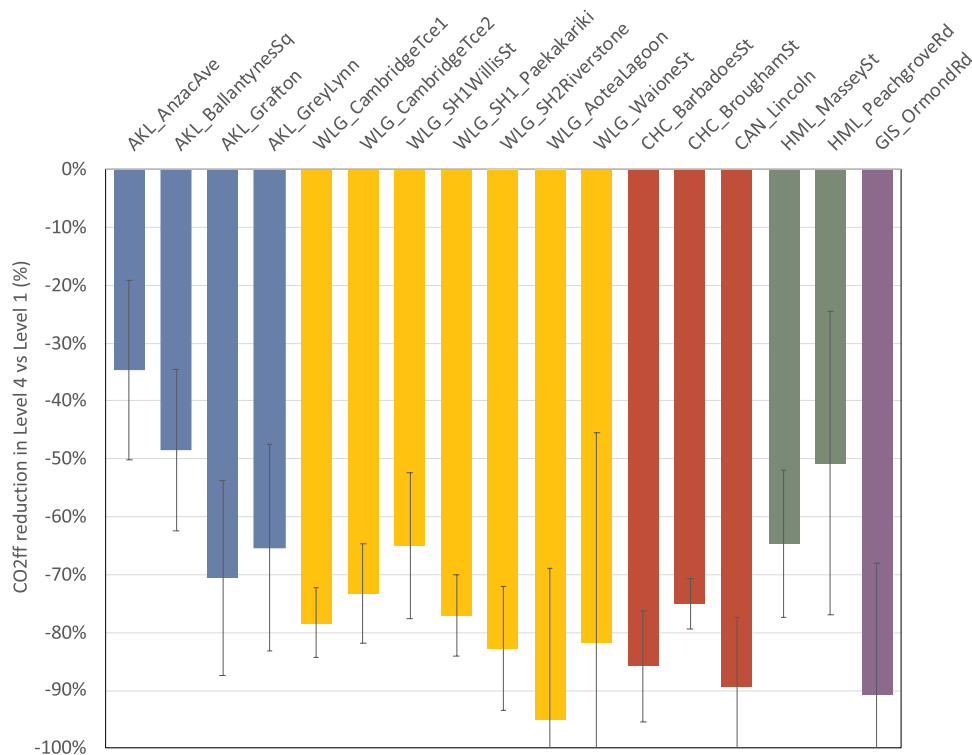
Figure 5. CO_{2ff} change in Level 4 lockdown relative to Level 1 at 17 sites around New Zealand, expressed as the reduction in CO_{2ff} mole fraction in Level 4 vs level 1. Error bars represent the calculated uncertainty in the emission reduction for each site.

within 20 m of busy roads, so the observed CO_{2ff} signals are expected to be dominated by traffic emissions (Figures S2 and S3). CO_{2ff} sources such as residential and commercial heating could also impact emissions at these sites, particularly since the lockdown required the vast majority of people to stay home during Level 4. Residential CO_{2ff} emissions are modest in New Zealand, representing 5% of urban CO_{2ff} emissions versus 40% from traffic under normal conditions[25] and are predominantly in the mornings and evenings[26] rather than daytime hours when

the grass is assimilating carbon. Wood burning is a relatively common residential heating source in New Zealand but does not contribute to CO_{2ff}.

One site located more than 100 m from the nearest road (WLG_GurneyRd, Figures 4 and S4) showed a trend broadly consistent with the patterns seen at other sites, but the CO_{2ff} mole fractions even during Level 1 were too small to diagnose changes through time and thus excluded from the dataset.

Second, day-to-day and synoptic scale meteorological variability such as changing wind direction and speed can result in large differences in CO_{2ff} mole fraction at the same location, even if the emission rate is constant. Yet for this study utilizing citizen science, we were unable to collect local meteorological information at each site. First, we considered whether seasonal changes in boundary layer height could bias our results, but only modest changes in daytime boundary layer height are observed in New Zealand cities during our sampling period from autumn (March−April−May) to winter (June−July−August).[27] Second, we evaluated the impact of meteorological variability at each site from the week-to-week variability in observed CO_{2ff} during the last few weeks of samples collected under Level 1 normal conditions. At most sites, the week-to-week variability in CO_{2ff} across all samples collected in Level 1 is no larger than the measurement uncertainty bounds (Figure 3 and Supporting Dataset). This indicates that week-to-week variability in meteorology did not significantly influence the observed CO_{2ff} mole fractions. Week-to-week changes in CO_{2ff} emission rate will therefore be proportional to week-to-week changes in CO_{2ff} mole fraction. Three sites did show substantial week-to-week differences in CO_{2ff} mole fraction during Level 1 and at other levels (AKL_FerndaleRd, WLG_SH2RiverRd, Figure 4). We hypothesize that at these two sites, specific local sources combined with week-to-week changes in wind patterns could drive the variability and these sites are excluded from further analysis. A third site, WLG_HuttRiverTaita, showed a pattern broadly consistent with traffic emissions, but a single observation during Level 1 showed a large discrepancy (Figure 4), which is most likely associated with a labeling error. Nonetheless, we excluded this site from further analysis.

Without explicit, detailed atmospheric transport information for each site, we still cannot infer absolute CO_{2ff} emission rates from the observed CO_{2ff} mole fractions, yet changes in the CO_{2ff} emission rate can be evaluated from the week-to-week change in observed CO_{2ff} mole fraction. This is simply done by determining the ratio of CO_{2ff}(Level 4) to CO_{2ff}(Level 1).

3. RESULTS

All sites show the lowest CO_{2ff} mole fractions during Level 4 (strictest lockdown restrictions), gradually increasing through Level 3, Level 2, and then staying consistent at higher values during Level 1 (normal) (Figure 3). A few outlier samples suggest unusual emissions during particular weeks or could also reflect sampling or labeling errors that are difficult to control for in a citizen science initiative.

The range of observed CO_{2ff} values varies by site, depending on proximity to and strength of local emission sources, with sites closest to busy roads showing higher CO_{2ff} mole fractions than sites further from emission sources. The drop in emissions during Level 4 compared to Level 1 varies by site from −36 to −99%, with a mean of −75 ± 3% across all 17 sites in five New Zealand regions (Figure 5). Our 17 sites encompass motorways, arterial routes, and urban and suburban streets from five different cities. This breadth of sites means that this small number of sites reasonably, but imperfectly, represent traffic emission changes across New Zealand.

Most sites are within 20 m of roads (Figures S2−S4), and therefore traffic emissions are the dominant emission source for these locations. In our observations, two sites in Auckland (AKL_ANZACAve and AKL_BallantynesSq) show smaller emission decreases during Level 4 than the other sites (−36 ± 19 and −50 ± 17%, Figures 3 and 5). AKL_ANZACAve is in a small park adjacent to a normally busy city street on a hill slope, surrounded by apartment buildings (Figure S1). This street is heavily trafficked by buses which continued to operate during Level 4 lockdown and is likely the reason for the smaller emission change. The site may also be influenced by nearby residential CO_{2ff} emissions, which are not expected to have dropped substantially during Level 4 lockdown. This result is consistent with a study of pollutants in central Auckland, suggesting that lockdown decreases in traffic-associated pollutants may have been more modest in the central business district than elsewhere, likely due to ongoing bus traffic in this area.[5,28]

Samples were also collected from two sites 100 m apart on Cambridge Terrace in the Wellington central business district, both on the median of the same divided city street (WLG_CambridgeTce1, WLG_CambridgeTce2, Figure 3). The first site is within 10 m of an intersection and shows a step change in CO_{2ff} mole fraction in Level 2, whereas the second site midway between intersections shows a more gradual increase in emissions through Level 2, as do all other sites in Wellington and around New Zealand (Figure 3). We hypothesize that in Level 2, the intersection became busy enough that traffic routinely backed up, resulting in a jump in emissions at this location. At the second site, traffic continued to flow, and vehicles did not idle close to the sampling site as often, resulting in a slower increase in emissions as people gradually resumed their normal travel (Figure 3).

4. DISCUSSION: COMPARISON WITH OTHER METRICS FOR EMISSION CHANGES

A global study of COVID-19-related CO_{2ff} emission changes based on proxy data[2] assigned surface transport emission reductions for Level 4 based on a combination of Apple Mobility data and TomTom urban congestion data. They determined a −47% change in traffic emissions for the "Oceania" region compromising New Zealand and Australia, substantially different than our observed decrease of −75 ± 3%. This is likely due to aggregating across two countries with different lockdown policies. The Apple mobility data for New Zealand alone (https://www.apple.com/covid19/mobility/) indicates a change in driving requests of −81% in Level 4 relative to the Level 1 recovery period. The slightly larger reduction in traffic implied by the Apple Mobility Data than in our CO_{2ff} observations could be because changes in driving requests are not an exact proxy for emission changes.[29]

Waka Kotahi New Zealand Transport Agency traffic count data shows a decrease in traffic counts during Level 4 relative to Level 1 of −75% in Auckland (two locations), −79% in Wellington, −74% in Christchurch, and −71% in Hamilton (https://opendata-nzta.opendata.arcgis.com/search?q=traffic). No traffic count data was available for Gisborne. In no case is the traffic count data co-located with our CO_{2ff} observations. On average, these traffic count data indicate a change in traffic of −75% during Level 4, consistent with our observed changes in CO_{2ff} emissions. However, our results demonstrate spatial variability in emission changes that is not captured by the traffic count data collected from fewer sites. Further, while traffic counts and traffic CO_{2ff} emissions are very strongly correlated during the 2020 COVID-19 lockdowns, it might be expected that as fuel efficiency improves and electric vehicles are more widespread in the near future, traffic counts and traffic CO_{2ff} emissions will decouple. This study demonstrates that roadside

[14]C sampling, either in grass or direct from atmospheric samples, could allow tracking of such changes.

5. CONCLUSIONS

Atmospheric observations of CO_{2ff} derived from ^{14}C content of grass samples demonstrated a $-75 \pm 3\%$ change in traffic emissions in New Zealand during the highest level of COVID-19 lockdown. This result is broadly consistent with changes in traffic counts, but the larger number of sampling sites reveals local differences in emission reductions. Our results demonstrate that while broad regional estimates are likely sufficient for inferring global emission changes, local studies such as ours are needed to elucidate the detail of local emission changes at a level relevant to policymakers. Our results show a strong relationship between changes in CO_{2ff} emissions and in traffic counts, and suggest that future decoupling of these two metrics, as fuel efficiency and electrification increase, could be observed through ^{14}C sampling in grass or direct atmospheric measurements.

Our inability to access the field combined with the population being kept at home created the perfect opportunity to engage citizens in science. Their contribution was an essential part of this project, proving to be an effective method to gather valuable and high-quality scientific information. The simplicity of the sample collection method, and participation of the public, proved to be an excellent route to public engagement in climate change and emissions mitigation.

ASSOCIATED CONTENT

Supporting Information

The Supporting Information is available free of charge at https://pubs.acs.org/doi/10.1021/acs.est.1c07994.

> Measurement precision and maps of each individual measurement site (PDF)
> Radiocarbon measurements and calculated CO_{2ff} for every measured sample (XLSX)

AUTHOR INFORMATION

Corresponding Author

Jocelyn C. Turnbull − *Rafter Radiocarbon Laboratory, GNS Science, Lower Hutt 5010, New Zealand; CIRES, University of Colorado at Boulder, Boulder, Colorado 80309, United States;* ⓘ orcid.org/0000-0002-0306-9658; Phone: +64 4 570 4726; Email: j.turnbull@gns.cri.nz

Authors

Lucas Gatti Domingues − *Rafter Radiocarbon Laboratory, GNS Science, Lower Hutt 5010, New Zealand*

Nikita Turton − *Rafter Radiocarbon Laboratory, GNS Science, Lower Hutt 5010, New Zealand*

Complete contact information is available at:
https://pubs.acs.org/10.1021/acs.est.1c07994

Notes

The authors declare no competing financial interest.

ACKNOWLEDGMENTS

REFERENCES

(1) Le Quéré, C.; Moriarty, R.; Andrew, R. M.; Peters, G. P.; Ciais, P.; Friedlingstein, P.; Jones, S. D.; Sitch, S.; Tans, P.; Arneth, A.; Boden, T. A.; Bopp, L.; Bozec, Y.; Canadell, J. G.; Chini, L. P.; Chevallier, F.; Cosca, C. E.; Harris, I.; Hoppema, M.; Houghton, R. A.; House, J. I.; Jain, A. K.; Johannessen, T.; Kato, E.; Keeling, R. F.; Kitidis, V.; Klein Goldewijk, K.; Koven, C.; Landa, C. S.; Landschützer, P.; Lenton, A.; Lima, I. D.; Marland, G.; Mathis, J. T.; Metzl, N.; Nojiri, Y.; Olsen, A.; Ono, T.; Peng, S.; Peters, W.; Pfeil, B.; Poulter, B.; Raupach, M. R.; Regnier, P.; Rödenbeck, C.; Saito, S.; Salisbury, J. E.; Schuster, U.; Schwinger, J.; Séférian, R.; Segschneider, J.; Steinhoff, T.; Stocker, B. D.; Sutton, A. J.; Takahashi, T.; Tilbrook, B.; van der Werf, G. R.; Viovy, N.; Wang, Y. P.; Wanninkhof, R.; Wiltshire, A.; Zeng, N. Global carbon budget 2015. *Earth Syst. Sci. Data* **2016**, *7*, 47−85.

(2) Le Quéré, C.; Jackson, R. B.; Jones, M. W.; Smith, A. J. P.; Abernethy, S.; Andrew, R. M.; De-Gol, A. J.; Willis, D. R.; Shan, Y.; Canadell, J. G.; Friedlingstein, P.; Creutzig, F.; Peters, G. P. Temporary reduction in daily global CO2 emissions during the COVID-19 forced confinement. *Nat. Clim. Change* **2020**, *10*, 647−653.

(3) Liu, Z.; Ciais, P.; Deng, Z.; Lei, R.; Davis, S. J.; Feng, S.; Zheng, B.; Cui, D.; Dou, X.; Zhu, B.; Guo, R.; Ke, P.; Sun, T.; Lu, C.; He, P.; Wang, Y.; Yue, X.; Wang, Y.; Lei, Y.; Zhou, H.; Cai, Z.; Wu, Y.; Guo, R.; Han, T.; Xue, J.; Boucher, O.; Boucher, E.; Chevallier, F.; Tanaka, K.; Wei, Y.; Zhong, H.; Kang, C.; Zhang, N.; Chen, B.; Xi, F.; Liu, M.; Breon, F. M.; Lu, Y.; Zhang, Q.; Guan, D.; Gong, P.; Kammen, D. M.; He, K.; Schellnhuber, H. J. Near-real-time monitoring of global CO2 emissions reveals the effects of the COVID-19 pandemic. *Nat. Commun.* **2020**, *11*, No. 5172.

(4) Bray, C. D.; Nahas, A.; Battye, W. H.; Aneja, V. P. Impact of lockdown during the COVID-19 outbreak on multi-scale air quality. *Atmos. Environ.* **2021**, *254*, No. 118386.

(5) Talbot, N.; Takada, A.; Bingham, A. H.; Elder, D.; Lay Yee, S.; Golubiewski, N. E. An investigation of the impacts of a successful COVID-19 response and meteorology on air quality in New Zealand. *Atmos. Environ.* **2021**, *254*, No. 118322.

(6) Potts, D. A.; Marais, E. A.; Boesch, H.; Pope, R. J.; Lee, J.; Drysdale, W.; Chipperfield, M. P.; Kerridge, B.; Siddans, R.; Moore, D. P.; Remedios, J. Diagnosing air quality changes in the UK during the COVID-19 lockdown using TROPOMI and GEOS-Chem. *Environ. Res. Lett.* **2021**, *16*, No. 054031.

(7) Brandao, R.; Foroutan, H. Air Quality in Southeast Brazil during COVID-19 Lockdown: A Combined Satellite and Ground-Based Data Analysis. *Atmosphere* **2021**, *12*, No. 583.

(8) Grange, S. K.; Lee, J. D.; Drysdale, W. S.; Lewis, A. C.; Hueglin, C.; Emmenegger, L.; Carslaw, D. C. COVID-19 lockdowns highlight a risk of increasing ozone pollution in European urban areas. *Atmos. Chem. Phys.* **2021**, *21*, 4169−4185.

(9) Turner, A. J.; Kim, J.; Fitzmaurice, H.; Newman, C.; Worthington, K.; Chan, K.; Wooldridge, P. J.; Köhler, P.; Frankenberg, C.; Cohen, R. C. Observed impacts of COVID-19 on urban CO_2 emissions. *Geophys. Res. Lett.* **2020**, *47*, No. e2020GL090037.

(10) Wu, S.; Zhou, W.; Xiong, X.; Burr, G. S.; Cheng, P.; Wang, P.; Niu, Z.; Hou, Y. The impact of COVID-19 lockdown on atmospheric CO2 in Xi'an, China. *Environ. Res.* **2021**, *197*, No. 111208.

(11) Velasco, E. Impact of Singapore's COVID-19 confinement on atmospheric CO2 fluxes at neighborhood scale. *Urban Clim.* **2021**, *37*, No. 100822.

(12) Yadav, V.; Ghosh, S.; Mueller, K.; Karion, A.; Roest, G.; Gourdji, S. M.; Lopez-Coto, I.; Gurney, K. R.; Parazoo, N.; Verhulst, K. R.; Kim, J.; Prinzivalli, S.; Fain, C.; Nehrkorn, T.; Mountain, M.; Keeling, R. F.; Weiss, R. F.; Duren, R.; Miller, C. E.; Whetstone, J. The Impact of COVID-19 on CO2 Emissions in the Los Angeles and Washington DC/Baltimore Metropolitan Areas. *Geophys. Res. Lett.* **2021**, *48*, No. e2021GL092744.

(13) Suess, H. E. Radiocarbon concentration in modern wood. *Science* **1955**, *122*, 414−417.

(14) Tans, P. P.; De Jong, A. F.; Mook, W. G. Natural atmospheric ^{14}C variation and the Suess effect. *Nature* **1979**, *280*, 826−828.

(15) Levin, I.; Kromer, B.; Schmidt, M.; Sartorius, H. A novel approach for independent budgeting of fossil fuel CO_2 over Europe by $^{14}CO_2$ observations. *Geophys. Res. Lett.* **2003**, *30*, No. 2194.

(16) Reimer, P. J.; Austin, W. E. N.; Bard, E.; Bayliss, A.; Blackwell, P. G.; Bronk Ramsey, C.; Butzin, M.; Cheng, H.; Edwards, R. L.; Friedrich, M.; Grootes, P. M.; Guilderson, T. P.; Hajdas, I.; Heaton, T. J.; Hogg, A. G.; Hughen, K. A.; Kromer, B.; Manning, S. W.; Muscheler, R.; Palmer, J. G.; Pearson, C.; van der Plicht, J.; Reimer, R. W.; Richards, D. A.; Scott, E. M.; Southon, J. R.; Turney, C. S. M.; Wacker, L.; Adolphi, F.; Büntgen, U.; Capano, M.; Fahrni, S. M.; Fogtmann-Schulz, A.; Friedrich, R.; Köhler, P.; Kudsk, S.; Miyake, F.; Olsen, J.; Reinig, F.; Sakamoto, M.; Sookdeo, A.; Talamo, S. The IntCal20 Northern hemisphere radiocarbon age calibration curve (0−55 CAL kBP). *Radiocarbon* **2020**, *62*, 725−757.

(17) Hsueh, D. Y.; Krakauer, N. Y.; Randerson, J. T.; Xu, X.; Trumbore, S. E.; Southon, J. R. Regional patterns of radiocarbon and fossil fuel-derived CO_2 in surface air across North America. *Geophys. Res. Lett.* **2007**, *34*, No. L02816.

(18) Turnbull, J. C.; Keller, E. D.; Norris, M. W.; Wiltshire, R. M. Independent evaluation of point source fossil fuel CO_2 emissions to better than 10%. *Proc. Natl. Acad. Sci.* **2016**, *113*, 10287−10291.

(19) Palstra, S. W. L.; Karstens, U.; Streurman, H.-J.; Meijer, H. A. J. Wine ethanol ^{14}C as a tracer for fossil fuel CO_2 emissions in Europe: Measurements and model comparison. *J. Geophys. Res.* **2008**, *113*, No. D21305.

(20) Shibata, S.; Kawano, E.; Nakabayashi, T. Atmospheric $[^{14}C]CO_2$ variations in Japan during 1982−1999 based on ^{14}C measurements of rice grains. *Appl. Radiat. Isot.* **2005**, *63*, 285−290.

(21) Bozhinova, D.; Combe, M.; Palstra, S. W. L.; Meijer, H. A. J.; Krol, M. C.; Peters, W. The importance of crop growth modeling to interpret the $^{14}CO_2$ signature of annual plants. *Global Biogeochem. Cycles* **2013**, *27*, 792−803.

(22) Turnbull, J. C.; Miller, J. B.; Lehman, S. J.; Tans, P. P.; Sparks, R. J.; Southon, J. R. Comparison of $^{14}CO_2$, CO and SF_6 as tracers for determination of recently added fossil fuel CO_2 in the atmosphere and implications for biological CO_2 exchange. *Geophys. Res. Lett.* **2006**, *33*, No. L01817.

(23) Turnbull, J. C.; Mikaloff Fletcher, S. E.; Ansell, I.; Brailsford, G. W.; Moss, R. C.; Norris, M. W.; Steinkamp, K. Sixty years of radiocarbon dioxide measurements at Wellington, New Zealand: 1954−2014. *Atmos. Chem. Phys.* **2017**, *17*, 14771−14784.

(24) Flesch, T. K.; Wilson, J. D.; Harper, L.; Crenna, B.; Sharpe, R. Deducing ground-to-air emissions from observed trace gas concentrations: A field trial. *J. Appl. Meteorol.* **2004**, *43*, 487−502.

(25) Xie, S. *Auckland's Greenhouse Gas Inventory to 2015*; ISSN 2230-4525 (Print) ISSN 2230-4533 (Online) ISBN 978-1-98-852960-8 (Print) ISBN 978-1-98-852961-5 (PDF); Auckland Council, 2017.

(26) Dortans, C.; Anderson, B.; Stephenson, J.; Jack, M. *Estimating the Technical Potential of Residential Demand Response in New Zealand: A Summary of Results*; GREENGrid Project Report, 2018.

(27) Marley, H. G.; Dirks, K. N.; McKendry, I.; Weissert, L. F.; Salmond, J. A. A Ceilometer-Derived Climatology of the Convective Boundary Layer Over a Southern Hemisphere Subtropical City. *Boundary-Layer Meteorol.* **2021**, *178*, 435−462.

(28) Patel, H.; Talbot, N.; Salmond, J.; Dirks, K.; Xie, S.; Davy, P. Implications for air quality management of changes in air quality during lockdown in Auckland (New Zealand) in response to the 2020 SARS-CoV-2 epidemic. *Sci. Total Environ.* **2020**, *746*, No. 141129.

(29) Gensheimer, J.; Turner, A. J.; Shekhar, A.; Wenzel, A.; Keutsch, F. N.; Chen, J. What are different measures of mobility telling us about surface transportation CO2 emissions during the COVID-19 pandemic? *J. Geophys. Res.: Atmos.* **2021**, *126*, No. e2021JD034664.